SCIENCE CHINA
Technological Sciences

• Article •

doi: 10.1007/s11431-016-9038-y

α→β Transformation characteristics revealed by pulsed laser-induced non-equilibrium microstructures in duplex-phase Zr alloy

CHAI LinJiang[1*], WANG ShuYan[1], Wu Hao[1], Guo Ning[2], Pan HuCheng[3], CHEN LiangYu[4], MURTY K. L.[5] & Song Bo[2*]

[1] *College of Materials Science and Engineering, Chongqing University of Technology, Chongqing 400054, China;*
[2] *Faculty of Materials and Energy, Southwest University, Chongqing 400715, China;*
[3] *Key Laboratory for Anisotropy and Texture of Materials (Ministry of Education), Northeastern University, Shenyang 110819, China;*
[4] *School of Mathematics and Science, Jiangsu University of Science and Technology, Jiangsu 212003, China;*
[5] *Department of Nuclear Engineering, North Carolina State University, Raleigh, NC 27695-7909, USA*

Received December 21, 2016; accepted March 13, 2017; published online May 17, 2017

Microstructures of a duplex-phase Zr-2.5Nb alloy treated by pulsed laser were characterized by electron backscatter diffraction (EBSD) and electron channeling contrast (ECC) imaging techniques. Major attention has been paid to non-equilibrium hybrid microstructure consisting of both prior α and β phases, and α plates transformed from new β phases to probe α→β transformation characteristics in the alloy. The origin of the hybrid microstructure is attributed to the specific thermodynamic conditions induced by the pulsed laser treatment. ECC observation shows that newly formed β phases during laser heating prefer to nucleate and grow at the expense of edges of prior α grains rather than their interiors. EBSD analyses further reveal that orientations of the new β phases are not determined by the prior α grains according to the Burgers relationship but maintain those of the prior β phases in an epitaxial growth way.

Zr alloy, microstructure, phase transformation, laser treatment, electron backscatter diffraction

Citation: Chai L J, Wang S Y, Wu H, et al. α→β Transformation characteristics revealed by pulsed laser-induced non-equilibrium microstructures in duplex-phase Zr alloy. Sci China Tech Sci, 2017, 60: doi: 10.1007/s11431-016-9038-y

1 Introduction

Zr alloys have long been accepted as key structural materials in the nuclear industry because of their low neutron absorption cross section, good corrosion resistance and mechanical properties [1]. Among commercially available ones, their microstructures could be essentially comprised of either single (α, with hexagonal close packed (hcp) structure) or duplex (α+β, the latter with body centered cubic (bcc) structure) phases after typical fabrications, leading to the category of single-phase and duplex-phase Zr alloys [2–7]. Zircaloy-2/4 belongs to the former while Zr-2.5Nb stands as a representative of the latter, which usually contains effective β-stabilizing Nb [8–10].

In practice, β-quenching treatments are often employed for both types of Zr alloys, with expectation to reach good homogenization of various alloying elements and alter crystallographic texture developed by earlier thermo-mechanical processing [11,12]. In regards to the α→β→α cycle involved, a number of efforts have been made to reveal microstructure and texture characteristics of the β→α transformation at cooling [13–17]. In contrast, much less has been known

*Corresponding authors (email: chailinjiang@cqut.edu.cn; bosong@swu.edu.cn)

on their α→β transformation characteristics at heating, due largely to the difficulty of characterizing microstructure and texture at elevated temperature. Although a few researchers have been able to perform *in situ* X-ray/neutron diffraction measurements on Zr alloys, they could only capture macro textures of α and β phases rather than specific microstructures [18,19]. Instead of resorting to such expensive procedures, one may expect to retain the high temperature microstructures at room temperature for performing regular characterization more easily. Such conserved microstructures will be thermodynamically unstable and hard to be attained through conventional heat treatments (such as furnace heating). However, the difficulty may be reduced by employing other methods (such as pulsed laser treatment [20,21]), which are capable of producing non-uniform thermal fields inducing various non-equilibrium microstructures. Assuming hybrid microstructures composed of transformed/untransformed α and β phases could be preserved at room temperature, the α→β transformation characteristics of Zr alloys would be feasibly revealed by regular characterization methods.

In the present work, a duplex-phase Zr-2.5Nb alloy was subjected to pulsed laser treatment with various modified microstructures examined using a field emission gun scanning electron microscope (FEGSEM). Particularly, detailed characterization was performed for a non-equilibrium hybrid microstructure consisting of both prior α and β phases and α plates transformed from new β phases. Results documented in this work are believed to be able to facilitate better recognition of α→β transformation characteristics in Zr alloys.

2 Materials and method

The as-received Zr-2.5Nb alloy (Zr-2.5 wt% Nb-0.1 wt% Fe-0.1 wt% O) was as-hot-deformed, with estimated transus temperatures of ~600, ~920 and ~1800 °C for α, β and liquid phases, respectively [12]. One specimen with dimensions of 15 mm×8 mm×3 mm in length, width and thickness directions (denoted as LD, WD and TD, respectively) was machined from the as-received material. LD-WD surface of the specimen was subjected to pulsed laser treatment utilizing a 600 W Nd: YAG laser device. The selected laser power was 100 W, with other operating parameters including 5 ms pulse width (or pulse frequency 20 Hz), +2 mm defocusing amount, 1 mm beam diameter, 8 mm/s beam travel speed along the LD in Ar gas atmosphere. Based on the selected parameters, energy and power densities of the laser treatment are 127.4 kW/mm^2 and 12.5 W s/mm, respectively.

A FEGSEM (Zeiss Sigma HD, Germany) equipped with an electron backscatter diffraction (EBSD) detector (Oxford Instruments NordlysMax2, UK) was employed to investigate microstructure and orientation characteristics of the laser-treated specimen. Softwares used for EBSD data acquisition and post-processing were AZtec 2.4 and HKL Channel 5, respectively. For direct microstructural observation, a technique of electron channeling contrast (ECC) imaging of backscattered electrons was mainly employed, which is known to be capable of revealing various crystallographic orientation-related defects [20,22], in addition to atomic-number (Z) contrast. Before both EBSD and ECC examinations, the specimen was mechanically ground using SiC paper and then electro-polished in mixed solution of 70 vol% methanol, 20 vol% butyl cellosolve and 10 vol% perchloric acid at −30 °C and 20 kV to obtain flat and stress free surfaces [23,24].

3 Results

3.1 The starting microstructure

Figure 1(a) is an ECC image showing the microstructure of the as-received Zr-2.5Nb material. Two types of morphologies are evident: the major one consisting of bulk grains in equiaxed or lamellar shape and the minor one corresponding to thin films surrounding the bulk grains. Considering phase constituent of the alloy [12,23], the bulk grains and the thin films are known to be α-Zr (majority) and β-Zr (minority), respectively. Different contrasts between α grains suggest varied orientations. The β films appear brighter than all α grains, which should be related to the Z contrast of backscattered electrons. The Z-contrast allows heavy elements (high Z) to be displayed brighter than light elements (low Z). For Zr-Nb alloys, β phases conserved at room temperature contain much higher Nb content (>10 wt%) than α phases (<0.6 wt%) [25,26]. Since Nb (Z=41) is slightly heavier than Zr (Z=40), the more enriched Nb should have led to the brighter contrast of the β films than the α grains. Also from Figure 1(a), grain sizes of α phases are found to be rather scattered, ranging from submicron to near ten micrometers. For the β films, on the other hand, their thicknesses are mainly limited to a few hundred nanometers, with an average value measured to be 72 nm.

EBSD indexing for both phases in this alloy was reported in earlier work to be a tough task, especially for the thin β films [27,28]. Nevertheless, they are satisfactorily resolved in this work, as testified in Figure 1(b) (a band contrast map with high image quality). Both phases are further clearly presented in an orientation imaging map (Figure 1(c)), with a black arrow indicating indexed β films. Figure 1(d) shows misorientation angle distribution of α grains revealing a large number of low angle boundaries (LABs, $2°<\theta<15°$). The abundance of the LABs is believed to result mainly from active dislocation slip during prior hot deformation. More specifically, further rotation axis analyses for these LABs suggest prismatic a slip ($\{10\bar{1}0\}/<11\bar{2}0>$) as the predominant slip system, as illustrated in our earlier work [23]. In addition to the LABs, a few high angle boundaries (HABs, $\theta>15°$) can also be seen

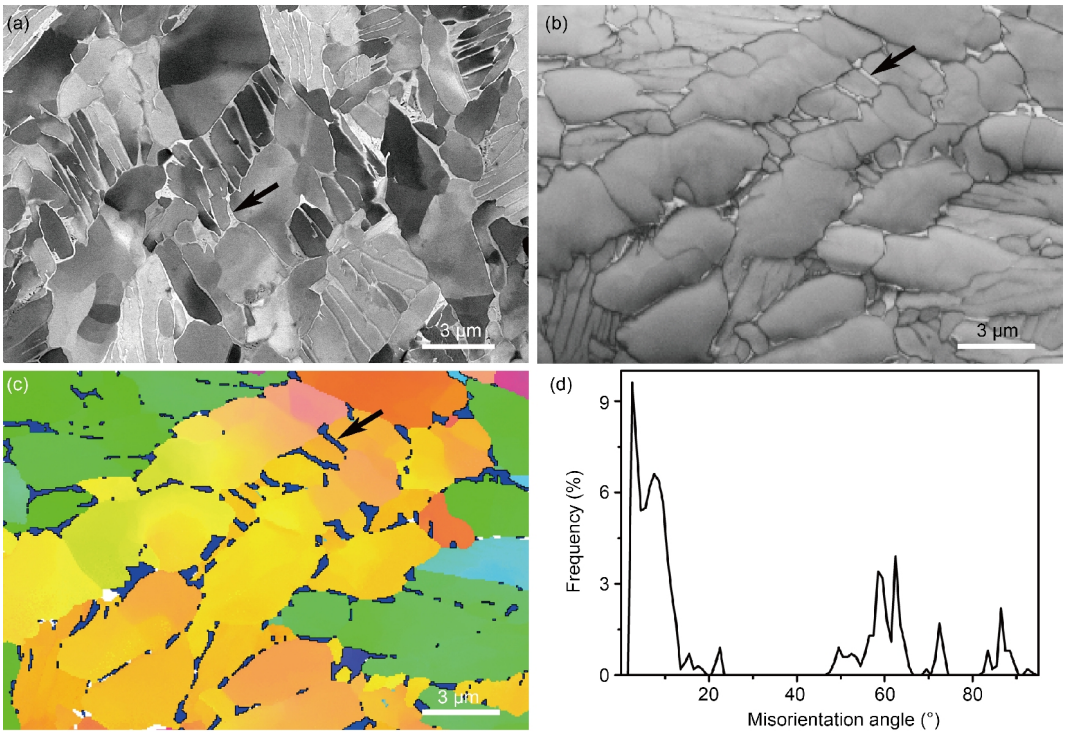

Figure 1 (Color online) Starting microstructure of the Zr-2.5Nb. (a) ECC image; (b) EBSD band contrast map; (c) orientation imaging map of both α and β phases corresponding to (b); (d) misorientation angle distribution histogram of α grains in (b). Arrows in (a)–(c) indicate β phases.

in Figure 1(d), confirming significant orientation variation suggested by ECC observation (Figure 1(a)).

3.2 The laser-induced microstructures

Figure 2 includes microstructures following laser treatment and Figure 2(a) is a low-magnification image where two dashed lines are added to indicate interfaces between modification zones of interest. The boxed region in Figure 2(a), crossing different modification zones, is magnified in Figure 2(b). The upper part in Figure 2(b) is found to be comprised of common α-plate structures with essentially uniform sizes that are clearly revealed by high-magnification observation (Figure 2(c)). That is why we denote this modification zone as uniform plate structure (UPS) zone. Figure 2(c) also reveals that dense nanotwins exist inside many α plates and their presence is believed to result from shear stresses during martensitic transformation induced by rapid cooling. Overall, such UPS is similar to that in conventionally β-water quenched Zr-2.5Nb alloy which has been extensively studied [14,29,30]. Beneath the UPS zone, three other types of morphologies are observed (jointly denoted as non-UPS zone), which are exemplified in Figure 2(d)–(f) corresponding to regions D, E and F in Figure 2(b), respectively. In contrast to the well-defined UPS, Figure 1(d) presents a bimodal α-plate structure (BPS) featured by relatively coarse plates as multiple cores surrounded by dense fine plates. Note that both the UPS and the BPS are fully comprised of α plates and the prior β phases are completely absent. A rough temperature gradient across both the α-plate-structure zones (such as regions C and D) is estimated to be >3.8 °C/μm. For region E (Figure 2(e)), however, although the prior bulk α phases are also transformed into plates, the β films seem to be nearly unaffected. In spite of interesting morphologies revealed in Figure 2(d) and (e), the disappearance of prior α grains hinders direct analyses on α→β transformation characteristics. The pulsed laser treatment is able to induce a hybrid microstructure of prior β phases, α plates (transformed from new β phases) and prior α grains towards the alloy matrix (Figure 2(f)). This is believed to be ideal for unraveling nucleation and growth features of new β phases relative to orientations and sites of both the prior α and β phases, as to be demonstrated in the following. The temperature gradient estimated for the latter two zones with prior β (e.g. regions C and D) is ~1.5 °C/μm.

Figure 3(a) is a significantly magnified image corresponding to the boxed region in Figure 2(f). One can clearly see that inside a prior α grain enclosed by continuous β films, edges of the grain are essentially replaced by fine α plates. As these plates could only be products of β→α cooling, these edge regions must be preferred nucleation sites of new β phases during heating, compared to the plate-free interior of the α grains. Figure 3(b) is a large EBSD band contrast map of such hybrid microstructure, covering the region observed in Figure 3(a) and thus allowing orientation characteristics of various structures to be determined. A small region of interest is extracted from Figure 3(b) (the white box) and analyzed in Figure 3(c)–

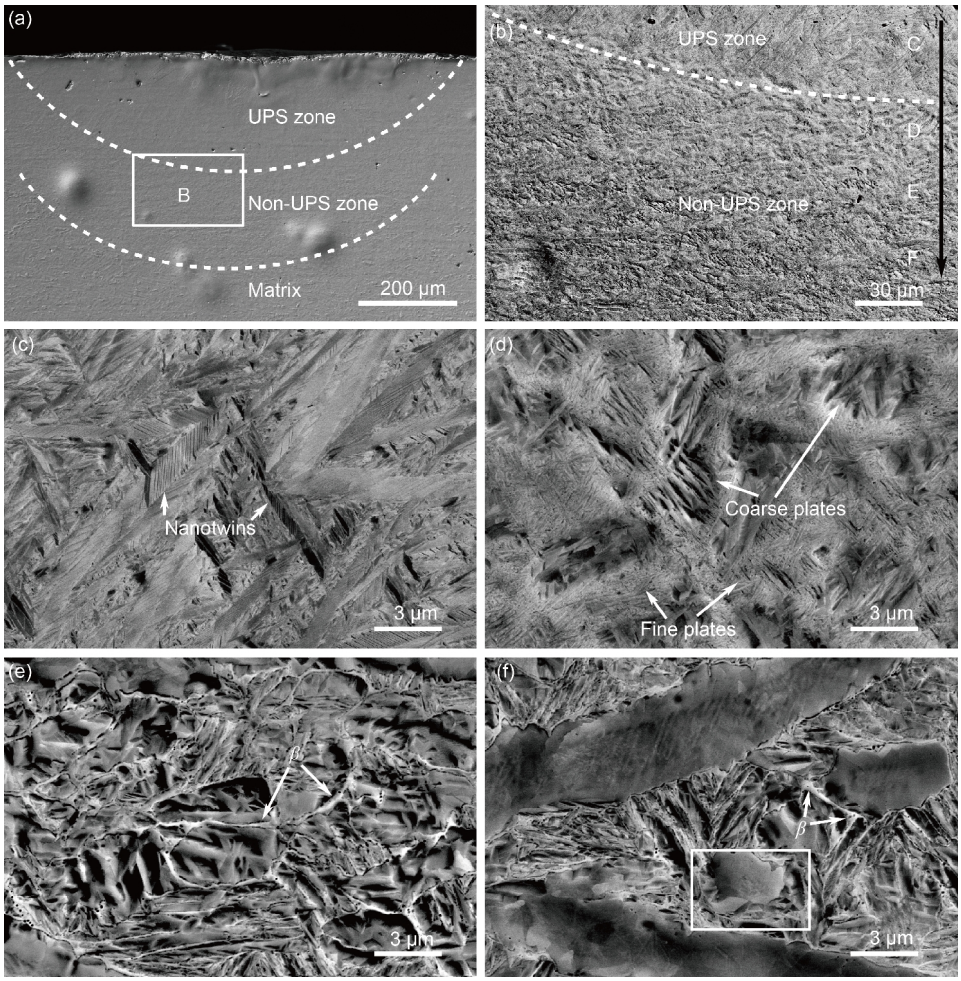

Figure 2 Overall microstructural observation on the laser-treated Zr-2.5Nb. (a) Cross-sectional view of the laser-modified regions at low magnification; (b) magnified image corresponding to box B in (a); (c)–(f) further magnified ECC images corresponding to regions C–F along the black arrow in (b). Dashed lines in (a) roughly distinguish different zones.

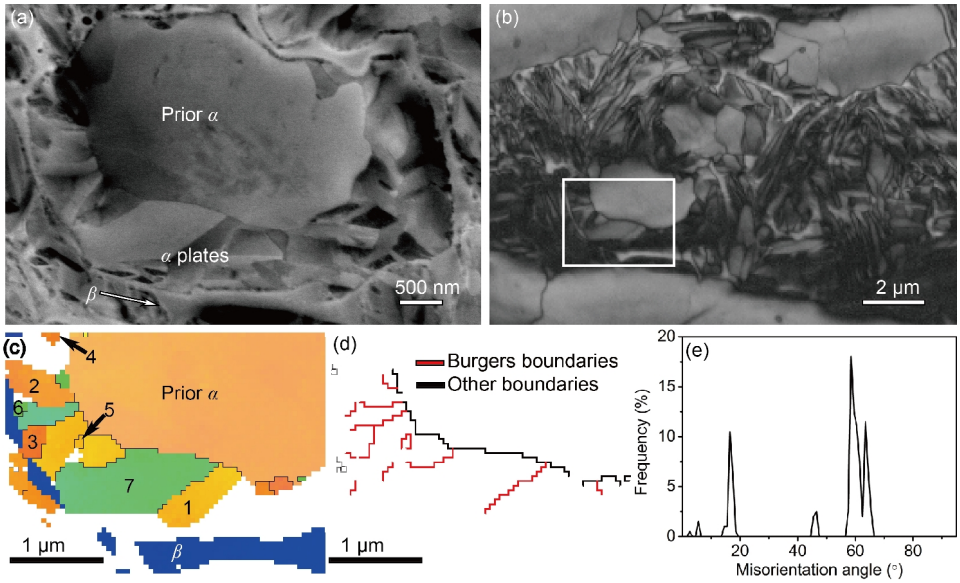

Figure 3 (Color online) (a) Closer ECC observation on the boxed region in Figure 2(f); (b) EBSD band contrast map corresponding to Figure 2(f); (c) orientation imaging map; (d) grain boundary map of α phases; (e) misorientation angle distribution histogram corresponding to the boxed region in (b). Consecutive numbers in (c) indicate different α variants transformed from a β orientation.

(e). In Figure 3(c), both the prior α and β show a single orientation while seven different orientations are noticed for transformed α plates, as marked by numbers. According to the Burgers relationship [31,32], 12 α-Zr variants could be produced by one β-Zr orientation and five possible misorientations (10.5°, 60°, 60.8°, 63.3° and 90°) exist between these α variants. α-Grain boundaries with and without the Burgers misorientations are depicted by different colors in Figure 3(d). One can see that all boundaries between the α plates examined in Figure 3(c) have the Burgers misorientations (particularly those around 60°–63° according to Figure 3(e)), suggesting that they are generated by the same β parent. On the contrary, none of these plates has Burgers boundaries with the prior α grain but suggests (Figure 3(e)) misorientation angles near 18° and 46° between them.

To further clarify orientation relationship between various structures in Figure 3(c), their crystallographic projection is presented in Figure 4. As the Burgers relationship predicts $\{110\}_\beta$ / $\{0001\}_\alpha$ and $< 111 >_\beta$ // $< 11\bar{2}0 >_\alpha$ [31], pole figures of {110} and {111} of the β-Zr and {0001} and $\{11\bar{2}0\}$ of the α-Zr are used to perform comparative analyses. Comparing Figure 4(a) and (b), one could find that projection sites in {0001} pole figure of most α orientations (except the one in the lower left quadrant) are coincident with those in {110} pole figure of the preexisting β phase. To make an easier comparison, all α orientations are separately projected in Figure 4(c)–(h). Clear projection deviation between Figure 4(a) and (c) indicates that the prior α grain in Figure 3(c) has no orientation relationship with the surrounded β film. In contrast, the Burgers relationship is found to exist between every α plate and the β orientation. For example, Figure 4(d) shows that basal planes of plates 1 and 2 are aligned parallel to each other (superposed symbols of circle and triangle) and their projection coincides with one of the six $\{110\}_\beta$ planes in Figure 4(a). Meanwhile, one of the three $< 11\bar{2}0 >$ planes for both plates is found accordingly coincident with one of the four $\{111\}_\beta$ planes. This testifies that the two α plates are definitely related to the prior β phase by the Burgers relationship and they are different variants generated by the same β orientation. In fact, Figure 4(d) also reveals a slight angular deviation (~10°) between $\{11\bar{2}0\}$ projections of the two variants, suggesting the Burgers misorientation of $10.5\,° / < 0001 >$. After making similar orientation analyses for other α plates, all of them can be confirmed to be variants generated by a β orientation identical with that of the prior β phase. In other words, the orientation of the β parent of α plates in Figure 3(c) seems to be determined by the surrounding preexisting β film rather than the prior α grain.

4 Discussion

In recent years, there have indeed been a few efforts attempted to probe α→β transformation characteristics of Zr alloys, especially by employing X-ray/neutron diffraction methods [18,19,33–35]. For single-phase Zr alloys (e.g. Zircaloy-2/4), Wenk et al. [34] and Romero et al. [19] reported occurrence of β variant selection during heating α phases, i.e. not all six β orientations theoretically predicted by the Burgers relationship from one α orientation would appear. For duplex-phase Zr alloys, however, the preexisting β phases may exert some effect on the α→β transformation at elevated temperature. For instance, Sattari et al. [35] suggested that in a duplex-phase Zr alloy Excel (Zr-3.5Sn-0.8Mo-0.8Nb) newly formed β phases during heating resulted from epitaxial growth of the preexisting β-Zr and thus perfectly inherited the original β orientations (texture). Nevertheless, Daymond et al. [18] argued that high temperature β phases in heated Zr-2.5Nb should mainly be generated through nucleation and growth inside α grains, similar to the case in Zircaloy-2/4 [19,34]. Such controversies in literature may be attributed to lack of explicit microstructural information provided by earlier researchers. In fact, to clarify this question, both the prior and the newly formed phases are better to be simultaneously characterized. Due to thermodynamic difference, it is hard to make them co-exist at room temperature through conventional heat treatments. While advanced electron microscopes fitted with special heating stages may enable *in situ* observation on high temperature microstructures [36], their expensive access fees have prevented researchers to reach better recognition on the above question.

In the present work, however, by employing pulsed laser to treat a Zr-2.5Nb, we are able to obtain non-equilibrium microstructures consisting of prior α and β phases, and α plates transformed from new β phases as well (Figures 2 and 3). As revealed in Figure 3(a), the newly formed β phase (parent of α plates) prefers to appear in the periphery (rather than the interior) of the prior α grain (adjacent to the preexisting β film). Figure 4 confirms that the parent of α plates owns identical orientation with the prior β phase but has no orientation relationship with the prior α grain, excluding possibility of the new β phase nucleating from the α grain by the Burgers relationship. These results strongly suggest that the α→β transformation in the duplex-phase Zr alloy is proceeded by epitaxial growth of prior β phases, evidencing those suggested by Sattari et al. [35].

In addition, the results presented in Figures 3 and 4 may also allow us to tentatively discuss effect of untransformed α phases on β→α transformation in the alloy. A strong texture memory effect was reported by different researchers [19,34] for heat treated Zr alloys with peak temperatures lower than β transus and attributed to the significant role played by untransformed (remnant) α phases in determining preferred α variants during cooling. However, Figure 4 in this work shows that none of orientations of the transformed

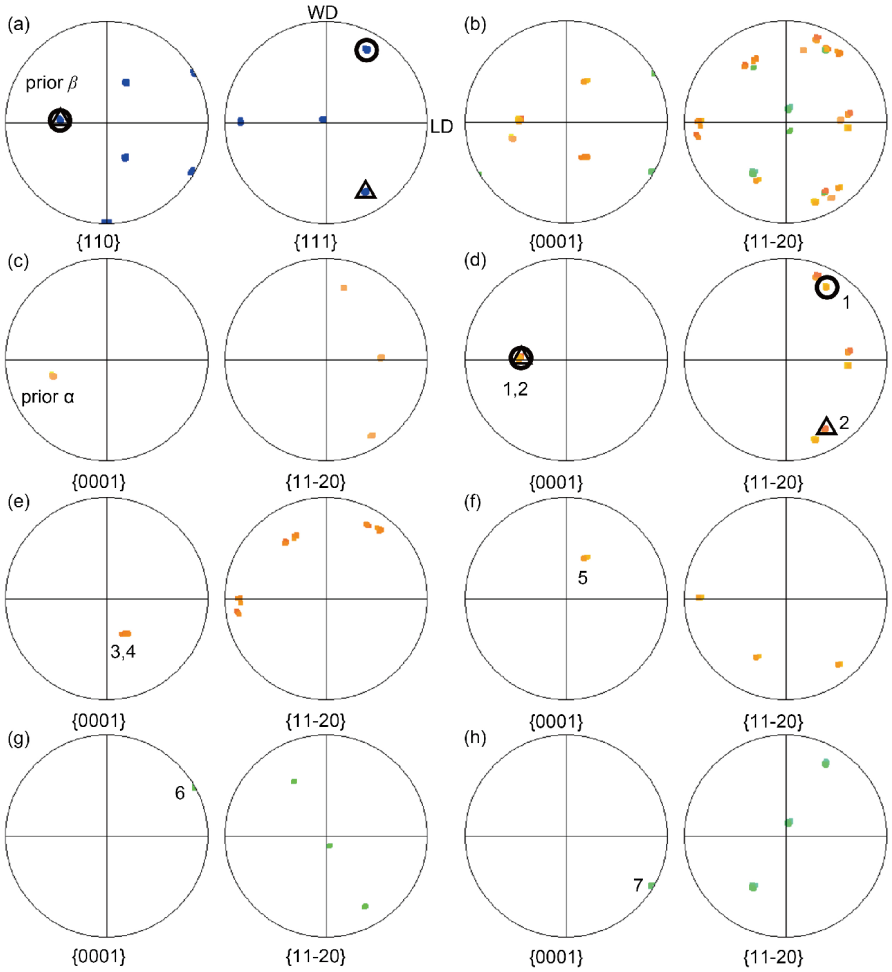

Figure 4 (Color online) Crystallographic projection corresponding to Figure 3(c). (a) {110} and {111} pole figures of the β film; (b) {0001} and {11$\bar{2}$0} pole figures of all α orientations; (c) the prior α orientation; (d)–(h) various α variants. Symbols in (a) and (d) indicate coincident projection of β and α orientations.

α plates is consistent with the prior α grain, which thus shows hardly any effect on the β→α process. The inconsistency with earlier work may lie in the fact that the remnant α phases in refs. [19,34] were already well related to high temperature β phases before β cooling, allowing further α variants with prior orientations to be preferably precipitated with energy advantage [37]. In contrast, the prior α and β orientations in Figure 3(c) are mutually non-Burgers related (due probably to previous hot deformation), hence such effect of the untransformed α phases is also lost.

In regards to origin of the above microstructures (Figure 2), we need to reconsider the non-equilibrium processing associated with the pulsed laser treatment in the present work. Different from conventional heat treatments, only a small volume of surface layer can be rapidly heated in laser-treated specimens, with the temperature gradient decreasing towards the alloy matrix (along the arrow in Figure 2(b)). Since the laser pulse is short (5 ms), the activated volume will be cooled down soon after transient heating. Nevertheless, the peak temperatures in regions C and D in Figure 2(b) could be high enough to allow Nb to diffuse. According to ref. [38], the diffusion coefficient (D) of Nb in β-Zr is extrapolated to be 1.6×10^{-12} m^2/s at 1500 °C. The 5 ms duration at such a high temperature gives a diffusion distance of about 180 nm (calculated by $2\sqrt{Dt}$ where t is the time), larger than the average thickness of β-films (72 nm). This means that relatively sufficient diffusion of Nb can take place. When the Nb content in preexisting β films is lower than ~10 wt% after diffusion, subsequent cooling is no longer able to conserve the prior β phases but transforms them into α plates [26]. By and large, the transformation involved in the UPS zones is believed to resemble that of conventional β solution treatment [14,29,30] while the presence of the BPS may be related to less homogeneous Nb distribution due to slightly lower temperature. For regions E and F in Figure 2(b), lower peak temperatures would lead to more limited Nb diffusion. For instance, D_{Nb} in β-Zr is measured to be 1.68×10^{-14} m^2/s at 900 °C [38], allowing only a diffusion distance of 18.4 nm for 5 ms. Therefore, no remarkable change is expected for the prior Nb-enriched β films that can be subsequently conserved. Accordingly, the newly formed β phases would be Nb-depleted and easily transformed into α plates after cooling

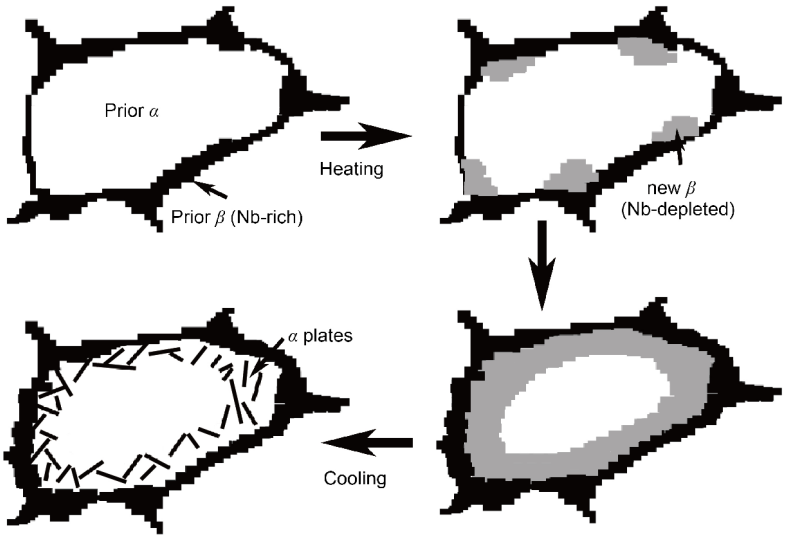

Figure 5 Schematic illustrating nucleation and growth of new β phases during pulsed laser heating and resultant α plates during cooling.

(Figure 2(e) and (f)). Those untransformed α grains in Figure 2(f) suggest that heat supplied by the pulsed laser is no longer sufficient for complete α→β transformation in locations deeper than about 350 μm from the surface.

After the above analyses, the formation of the non-equilibrium microstructure in Figure 3 can be schematically illustrated in Figure 5, which also clarifies the α→β transformation features in the pulsed laser-induced Zr-2.5Nb alloy. Initial heating induced by the pulsed laser allows new β phases to nucleate from the preexisting β films. However, limited heat due to the short pulse only allows highly restricted Nb diffusion so that the prior and the new β phases are Nb-rich and Nb-depleted, respectively. The limited heat may also allow the new β nuclei to slightly grow in an eptiaxial way but not to annex the entire prior α grain. In subsequent cooling, the Nb-rich prior β phases are still conserved while the Nb-depleted new β phases are transformed into α plates according to the Burgers relationship.

5 Conclusions

A non-equilibrium hybrid microstructure consisting of both prior α and β phases and α plates transformed from new β phases is induced by pulsed laser in a duplex-phase Zr-2.5Nb alloy. Newly formed β phases during laser heating prefer to nucleate and grow at the expense of edges rather than interiors of prior α grains. Orientations of the new β phases are not determined by the prior α grains according to the Burgers relationship but maintain those of the prior β phases in an eptiaxial growth way.

This work was supported by the National Natural Science Foundation of China (Grant No. 51401040), China Postdoctoral Science Foundation (Grant No. 2015M572446), Postdoctoral Science Foundation of Chongqing (Grant No. Xm2015003), and Scientific and Technological Research Program of Chongqing Municipal Education Commission (Grant No. KJ1500901).

1 Zinkle S J, Was G S. Materials challenges in nuclear energy. Acta Mater, 2013, 61: 735–758
2 Chai L, Luan B, Murty K L, et al. Twinning during recrystallization cooling in α-Zr alloy. Mater Sci Eng-A, 2013, 576: 320–325
3 Chen L, Zeng Q, Li J, et al. Effect of microstructure on corrosion behavior of a Zr-Sn-Nb-Fe-Cu-O alloy. Mater Des, 2016, 92: 888–896
4 Chai L, Luan B, Xiao D, et al. Microstructural and textural evolution of commercially pure Zr sheet rolled at room and liquid nitrogen temperatures. Mater Des, 2015, 85: 296–308
5 Liang J, Zhang M, Ouyang Y, et al. Contribution on the phase equilibria in Zr-Nb-Fe system. J Nucl Mater, 2015, 466: 627–633
6 Hiwarkar V D, Sahoo S K, Mani krishna K V, et al. Coarsening of second phase in a two-phase Zr-2.5Nb: On the role of phase boundaries. Acta Mater, 2009, 57: 5812–5821
7 Yang Z N, Zhang F C, Qu L, et al. Formation of duplex microstructure in Zr-2.3Nb alloy and its plastic behaviour at various strain rates. Int J Plasticity, 2014, 54: 163–177
8 Northwood D O, Lim D T. Phase transformations in zirconium and its alloys. Canadian Metall Q, 1979, 18: 441–467
9 Feng Z H, Jiang X J, Zhou Y K, et al. Influence of beryllium addition on the microstructural evolution and mechanical properties of Zr alloys. Mater Des, 2015, 65: 890–895
10 Yang H L, Kano S, Matsukawa Y, et al. Effect of molybdenum on microstructures in Zr-1.2Nb alloys after β-quenching and subsequently 873 K annealing. Mater Des, 2016, 104: 355–364
11 Dahlbäck M, Limbäck M, Hallstadius L, et al. The effect of beta-quenching in final dimension on the irradiation growth of tubes and channels. J ASTM Int, 2005, 2: 276–304
12 Li Y, Rogge R, Holt R A. Development of local microstructure and crystallographic texture in extruded Zr-2.5Nb tubes. Mater Sci Eng-A, 2006, 437: 10–20
13 Massih A R, Andersson T, Witt P, et al. Effect of quenching rate on the β-to-α phase transformation structure in zirconium alloy. J Nucl Mater, 2003, 322: 138–151
14 Srivastava D, Mukhopadhyay P, Banerjee S, et al. Morphology and substructure of lath martensites in dilute ZrNb alloys. Mater Sci Eng-A, 2000, 288: 101–110
15 Kim H G, Baek J H, Kim S D, et al. Microstructure and corrosion

characteristics of Zr-1.5Nb-0.4Sn-0.2Fe-0.1Cr alloy with a β-annealing. J Nucl Mater, 2008, 372: 304–311
16 Ben Ammar Y, Aoufi A, Darrieulat M. Influence of the cooling rate on the texture and the microstructure of Zircaloy-4 studied by means of a Jominy end-quench test. Mater Sci Eng-A, 2012, 556: 184–193
17 Gey N, Humbert M, Gautier E, et al. Study of the β→α variant selection for a zircaloy-4 rod heated to the β transus in presence or not of an axial tensile stress. J Nucl Mater, 2004, 328: 137–145
18 Daymond M R, Holt R A, Cai S, et al. Texture inheritance and variant selection through an hcp-bcc-hcp phase transformation. Acta Mater, 2010, 58: 4053–4066
19 Romero J, Preuss M, Quinta da Fonseca J. Texture memory and variant selection during phase transformation of a zirconium alloy. Acta Mater, 2009, 57: 5501–5511
20 Chai L, Chen B, Wang S, et al. Microstructural changes of Zr702 induced by pulsed laser surface treatment. Appl Surface Sci, 2016, 364: 61–68
21 Chai L, Chen B, Wang S, et al. Microstructural characteristics of a commercially pure Zr treated by pulsed laser at different powers. Mater Charact, 2015, 110: 25–32
22 Zaefferer S, Elhami N N. Theory and application of electron channelling contrast imaging under controlled diffraction conditions. Acta Mater, 2014, 75: 20–50
23 Chai L J, Wang S Y, Luan B F, et al. Electron backscatter diffraction investigation of duplex-phase microstructure in a forged Zr-2.5Nb alloy. Sci China Tech Sci, 2016, 59: 673–679
24 Chai L, Chen B, Zhou Z, et al. A special twin relationship or a common Burgers misorientation between α plates after β quenching in Zr alloy? Mater Charact, 2015, 104: 61–65
25 Kim H G, Park J Y, Jeong Y H. Phase boundary of the Zr-rich region in commercial grade Zr-Nb alloys. J Nucl Mater, 2005, 347: 140–150
26 Choo K N, Kang Y H, Pyun S I, et al. Effect of composition and heat treatment on the microstructure and corrosion behavior of Zr-Nb alloys. J Nucl Mater, 1994, 209: 226–235
27 Hiwarkar V D, Sahoo S K, Samajdar I, et al. Annealing of cold worked two-phase Zr-2.5Nb: Associated microstructural developments. J Nucl Mater, 2009, 384: 30–37
28 Hovington P, Pinard P T, Lagacé M, et al. Towards a more comprehensive microstructural analysis of Zr-2.5Nb pressure tubing using image analysis and electron backscattered diffraction (EBSD). J Nucl Mater, 2009, 393: 162–174
29 Banerjee S, Krishnan R. Martensitic transformation in zirconium-niobium alloys. Acta Metall, 1971, 19: 1317–1326
30 Srivastava D, Madangopal K, Banerjee S, et al. Self accomodation morphology of martensite variants in Zr-2.5wt%Nb alloy. Acta Metall Mater, 1993, 41: 3445–3454
31 Burgers W G. On the process of transition of the cubic-body-centered modification into the hexagonal-close-packed modification of zirconium. Physica, 1934, 1: 561–586
32 Chai L, Luan B, Zhang M, et al. Experimental observation of 12 α variants inherited from one β grain in a Zr alloy. J Nucl Mater, 2013, 440: 377–381
33 Gey N, Gautier E, Humbert M, et al. Study of the α/β phase transformation of Zy-4 in presence of applied stresses at heating: Analysis of the inherited microstructures and textures. J Nucl Mater, 2002, 302: 175–184
34 Wenk H R, Lonardelli I, Williams D. Texture changes in the hcp→bcc→hcp transformation of zirconium studied *in situ* by neutron diffraction. Acta Mater, 2004, 52: 1899–1907
35 Sattari M, Holt R A, Daymond M R. Variant selection and transformation texture in zirconium alloy Excel. J Nucl Mater, 2014, 453: 120–123
36 Seward G G E, Celotto S, Prior D J, et al. *In situ* SEM-EBSD observations of the hcp to bcc phase transformation in commercially pure titanium. Acta Mater, 2004, 52: 821–832
37 Cayron C. Importance of the α→β transformation in the variant selection mechanisms of thermomechanically processed titanium alloys. Scripta Mater, 2008, 59: 570–573
38 Tiwari G P, Sharma B D, Raghunathan V S, et al. Self- and solute-diffusion in dilute zirconium-niobium alloys in β-phase. J Nucl Mater, 1973, 46: 35–40